

# **Shallow–crustal magma chamber beneath the axial high of the Coaxial Segment of Juan de Fuca Ridge at the "source site" of the 1993 eruption**

William Menke

Lamont–Doherty Earth Observatory of Columbia University, Palisades NY 10964 USA

Michael West

Lamont–Doherty Earth Observatory of Columbia University, Palisades NY 10964 USA

Maya Tolstoy

Lamont–Doherty Earth Observatory of Columbia University, Palisades NY 10964 USA

(07–December–01)

## **ABSTRACT**

Seismic imaging reveals a shallow–crustal magma chamber beneath the source site of the 1993 eruption on Coaxial segment, Juan de Fuca Ridge. The magma chamber is at least 6 km<sup>3</sup> in volume and contains at least 0.6 km<sup>3</sup> of melt, enough to supply at least several eruptions of a size equal to the one in 1993. No mid–crustal connection of this magma chamber with the magmatic plumbing of nearby Axial volcano (the current expression of the Cobb–Eickelberg hotspot) is evident, confirming previous geochemical and geological studies that argued against mixing between the two. The lack of connectivity implies that magma transport through the uppermost mantle and lower crust are very highly focused into narrow (<5–10 km) conduits.

## **INTRODUCTION**

The Coaxial segment of the intermediate–spreading–rate Juan de Fuca Ridge extends from about 5 to about 80 km north from the summit caldera of Axial volcano, the most recent of the Cobb–Eickelberg chain of volcanoes (Fig. 1). The Coaxial segment occupies an en echelon position with respect to the north rift of Axial volcano. Magmatism and resulting crustal accretion of the north rift and Axial volcano overlap for about 15 km. This area is one in which both ridge and hotspot processes are occurring in very close proximity.

Both Axial volcano and the Coaxial segment have been sites of recent volcanic eruptions. In 1993, a dike propagated from a bathymetric high (the so called "source site," at 46.17°N) near the southern end of the Coaxial segment to a distance of about 40 km to the north (Butterfield et al., 1997; Embley et al., 2000). In 1998, a dike propagated from near the Axial caldera to a point about 50 km to the south (Dziak and Fox, 1999). The propagation of both dikes was monitored by hydroacoustic tracking of the numerous microearthquakes that they caused (Dziak and Fox, 1999; Fox et al., 1995). The 1998 eruption caused 3 m of subsidence of the Axial caldera (Fox, 1999) and is thought to be associated with the central magma chamber that has been imaged beneath that volcano (West et al., 2001). The distribution of lava flows along the Coaxial segment and their chemistry, which is distinct from that of Axial basalts, have been used to argue that the source of the Coaxial lavas is distinct from the Axial magma chamber (Embley et al., 2000). Our seismic images are consistent with these inferences, and we argue that the 1993 eruption most likely originated in a shallow–crustal magma chamber located beneath the source site. This magma chamber is distinct from, and apparently unconnected to, the Axial magma chamber.

## ACQUISITION, PROCESSING, AND INTERPRETATION OF SEISMIC DATA

The data that we present here is from a 1999 active seismic experiment that was primarily focused on imaging the Axial magma chamber (West et al., 2001). About 5000 shots from R/V *Maurice Ewing's* airgun array (20 guns totaling 142 L) were recorded on six ocean–bottom seismometers (OBSs) (Webb, 1998) deployed on the volcano's flanks. Water–wave traveltimes and Global Positioning System–determined shot locations were used to precisely locate the OBS's on the sea floor (error < 20 m) and to determine clock drifts (error < 0.02 s). The dense record sections permitted the identification of the major compressional waves, including the crustal turning Pg, Moho reflected PmP, and mantle refracted Pn. Although many lines of shots were recorded during this experiment, four lines in particular, recorded by two

OBSs located just north of Axial volcano, are relevant to this discussion of the Coaxial segment.

Line 1 crosses the Coaxial segment source Site at  $46.18^{\circ}\text{N}$ . A distinct shadow zone and Pg arrivals delayed by 0.1–0.3 s are evident on record sections from both OBS 1 and OBS 2, at source–OBS ranges of 14–20 km (Fig. 2, bottom). These features occur at just those positions along line 1 where the Pg waves pass beneath the source site. We infer that the Pg waves are interacting with a low–compressional–velocity zone (LVZ) associated with a magma chamber at that location. In order to accept this interpretation, the possibility that the delayed arrivals are actually deeper PmP Moho reflections must be discounted. A record section from line 2 to OBS 2, which has Pg waves that miss the Coaxial segment, provides the necessary evidence (Fig. 2, top right). No shadow zones or delayed arrivals are evident on this line, even though it has the same source–OBS ranges (5–20 km) as line 1. PmP reflections are seen on record sections (not shown) for line 4 to OBS 1, which sample crust to the east of the Coaxial segment. These reflections start at about 25 km range (corresponding to a crustal thickness of about 8 km), suggesting that confusion of PmP with delayed Pg ought not to be a problem for line 1’s shorter ranges. Finally, line 3 crosses the very southernmost part of the Coaxial segment at  $46.12^{\circ}\text{N}$ . No shadow zones or delayed arrivals are evident on record sections from this line, indicating that the Coaxial magma chamber does not extend this far south.

Some insight into the dimensions of the magma chamber can be gained by simple, forward modeling of the traveltimes of line 1. We began with a three–dimensional model of the region in which the velocity field was parameterized on an irregular tetrahedral grid; the prescribed water velocity and bathymetry were drawn from multibeam sonar measurements. The velocity field was initially a best–fitting one–dimensional structure, draped onto the bathymetry. We then perturbed this velocity field with a LVZ located beneath the Coaxial segment. The position of the delayed arrivals on line 1 placed strong constraints on the size and position of the LVZ along the segment: its southern end must be near  $46.12^{\circ}\text{N}$  and it must extend at least 3 km northward; its width must be about 2 km; and the low velocities must occur at least at 4–5 km

below sea level (about 2–3 km below seafloor). The data are not able to distinguish whether the LVZ persists north of 46.15°N, nor to detect whether it extends beneath 5 km depth below seafloor. The minimum velocity required depends on how the velocity is assumed to vary within the perturbed area. A model in which it linearly decreases toward the center of the perturbation requires a minimum velocity of about 3 km/s (Fig. 3). The Coaxial magma chamber is similar in width and overall traveltime delay to the ones on the fast–spreading East Pacific Rise at 9.50°N (Toomey et al., 1990) and at 13.00°N (Harding et al., 1989).

A tomographic inversion was also performed, on data from all lines and OBSs (16,700 Pg traveltimes), including those around Axial volcano. Traveltimes and their Frechet derivatives were calculated by using ray theory, and a linearized damped least–squares method was used to update the velocity field. Three iterations of the inversion were performed, starting with the bathymetrically draped one dimensional model, that resulted in a 54% reduction of the root–mean–square traveltime error. The final three–dimensional velocity field clearly reproduces all of the features evident from the simpler analysis (Fig. 4). Of particular interest is the lack of connectivity of the Coaxial and Axial magma chambers, at least at mid–crustal depths. The two magma chambers are separated by about 10 km of basalt with normal compressional velocities (in the 6.0–6.5 km/s range) that show no sign of containing magma. Checkerboard–style resolution tests (not shown) indicate that the spatial resolution of the inversion is sufficiently good in the critical region between the two magma chambers to detect connectivity, if it existed in the depth range of 2–6 km below sea level.

## RESULTS AND CONCLUSIONS

The imaged part of the Coaxial magma chamber has a minimum volume of about 6 km<sup>3</sup>. Although the relationship between seismic velocity decrease and melt fraction is imprecisely known, we estimate a minimum of 10% melt on the basis of laboratory and theoretical studies of Takei (1998), Sato et al. (1989), and Christensen (1979). The imaged part

of the magma chamber thus contains a minimum of about  $0.6 \text{ km}^3$  of melt, sufficient to produce about four dikes of the size of the 1993 dike (with the 1 m width discussed by Embley et al., 2000). The magma chamber can supply crust at a 5.5 cm/yr spreading rate for at least 40 yr, and perhaps longer, given that the magma chamber may extend northward out of the imaged area.

Two lines of reasoning suggest that the magma chamber may extend northward to about  $46.20^\circ\text{N}$  (i.e. a total length of 5–6 km). The axial high, which represents the magmatically most robust part of the segment, extends to about there. Furthermore, the southernmost earthquakes associated with the 1993 dike propagation occurred at about  $46.20^\circ\text{N}$ . They may mark the point at the north end of the magma chamber at which the dike began. The total volume of melt in the magma chamber may therefore be about  $1 \text{ km}^3$ .

The 1993 dike propagated steadily over a three-day period from the the source site to the so-called flow site, 40 km further north (at  $46.53^\circ\text{N}$ ), where it surfaced as a lava flow (Fox et al., 1995). The steady propagation strongly suggests that no further magma chambers occur along this 40 km length of the Coaxial segment, because such features would act to reduce the stress at the dike tip and to slow its propagation. There appears to be no source of magma farther north along the Coaxial segment that could recharge the magma chamber. Recharge from the nearby Axial volcano magma chamber (West et al., 2001), which is only 10–15 km away, is in our opinion unlikely for several reasons: First, Axial and Coaxial lavas have distinct  $^{87}\text{Sr}/^{86}\text{Sr}$  and  $^{143}\text{Nd}/^{144}\text{Nd}$  ratios that are consistent with their being from distinct mantle sources (Embley et al., 2000), and inconsistent with their having been drawn from a single, well-mixed magma chamber or even from a zoned magma chamber produced through differentiation of a single parent magma. Second, recharge from Axial volcano's magma chamber would presumably be via shallow (<5 km) lateral diking through the Helium Basin (Fig. 1). This topographically low basin appears magmatically starved, with no young volcanic features occurring near where it adjoins Axial volcano. In contrast, Axial's northern rift zone, a topographically high region located 10 km west of the Coaxial segment, is known to have young lavas with an Axial

geochemical affinity (Smith, 1999). Its smooth northward deepening from where it connects to Axial is consistent with its being a constructional Axial volcano–fed volcanic feature. Dike injection from the Axial magma chamber to the north thus seems to be focused well west of Coaxial segment. Finally, the Coaxial and Axial magma chambers appear to be unconnected on the seismic images. We are therefore led to conclude that the Coaxial magma chamber is being recharged from a mantle source below. The mantle sources of the hotspot–related Axial volcano and Coaxial segment of the Juan de Fuca Ridge thus appear to be separated horizontally by only 10–20 km and yet have remained chemically distinct. Magma transport through the melt generation region of the uppermost mantle (which extends to at least 75 km depth) must, when magma reaches the base of the crust, be focused to horizontal–length scales of only 5–10 km, which is to say into relatively narrow conduits.

#### ACKNOWLEDGEMENTS

We thank V. Ballu, D. Bohnenstiehl, J. Floyd, C. Goldenthe, R. Sohn, S. Webb and the crews of R/V *Maurice Ewing* and R/V *Thomas G. Thompson* for their efforts at sea, and R. Sohn and S. Webb for their efforts with the OBS instrumentation. Tomographic imaging was performed by W. Menke’s freely–available Raytrace3d software. This research was supported by the National Science Foundation. Lamont–Doherty Contribution Number 0000.

#### REFERENCES

Butterfield, D., Johnson, I.R., Massoth, G.J., Feely, R.A., Roe, K.K., Embley, R.W. Holden, J.F., McDuff, R.E. Lilley, M.D. and Delaney, J.R., 1977. Seafloor eruptions and evolution of hydrothermal fluid chemistry: *Philosophical Transactions of the Royal Society of London, Series A.*, v. 355, p. 369–386.

Christensen, N.I., 1979, Compressional wave velocities in rocks at high temperatures and pressures, critical thermal gradients, and crustal low-velocity zones: *Journal of Geophysical Research*, v. 84, p. 6849–6857.

Dziak, R.P. and Fox, C.G., 1999, The January 1998 earthquake swarm at Axial Volcano, Juan de Fuca Ridge, Hydroacoustic evidence for seafloor volcanic activity: *Geophysical Research Letters*, v. 26, p. 3425–3428.

Embley, R.W., Chadwick, W.W., Perfit, M.R., Smith, M.C. And Delaney, J.R., 2000, Recent Eruptions on the Coaxial segment of the Juan de Fuca Ridge: Implications for mid-ocean ridge accretion processes: *Journal of Geophysical Research*, v. 105, p. 16501–16525.

Fox, C.G., 1999, In situ ground deformation measurements from the summit of Axial Volcano during the 1998 volcanic episode: *Geophysical Research Letters*, v. 26, p. 3437–3440.

Fox, C.G. Radford, W.E., Dziak, R.P., Lau, T.K., Matsumoto, H. and Schriener, A.E., 1995, Acoustic detection of a seafloor presading episode on the Juan de Fuca Ridge using military hydrophone arrays: *Geophysical Research Letters*, v. 22, p. 131–134.

Harding, A.J., Orcutt, J.A., Kappus, M.E., Vera, E.E., Mutter, J.C., Buhl, P., Detrick. R.S. and Brocher, T.M., 1989: Structure of young oceanic crust at 13N on the East Pacific Rise from expanding spread profiles, *Journal of Geophysical Research*, v. 94, p. 12163–12196.

Sato, H., Sacks, S.I. And Murase, T., 1989, The use of laboratory velocity data for estimating temperature and partial melt fraction in the low-velocity zone; comparison with heat flow and

electrical conductivity study: *Journal of Geophysical Research*, v. 94, p. 5689–5704.

Smith, M.C., 1999, *Geochemistry of eastern Pacific MORB: Implications for MORB petrogenesis and the nature of crustal accretion within the neovolcanic zone of two recently active ridge segments* [Ph.D. Thesis]: Gainesville, University of Florida, p. 255.

Takei, Y., 1998, Constitutive mechanical relations of solid–liquid composites in terms of grain–boundary contiguity: *Journal of Geophysical Research*, v. 103, p. 18183–18203.

Toomey, D.R., G.M. Purdy, S.C. Solomon & W.S.D. Wilcock, 1990, The three–dimensional seismic velocity structure of the East Pacific Rise near latitude 9:30°N: *Nature*, v. 347, p. 639–644.

Webb, S.C., *Broadband seismology and noise under the ocean: Reviews of Geophysics*, v. 36, 105–142, 1998.

West, M., Menke, W. Tolstoy, M., Webb, S. and Sohn, R., 2001, Magma storage beneath Axial volcano on the Juan de Fuca mid–ocean ridge: *Nature* v. 25, p. 833–837.

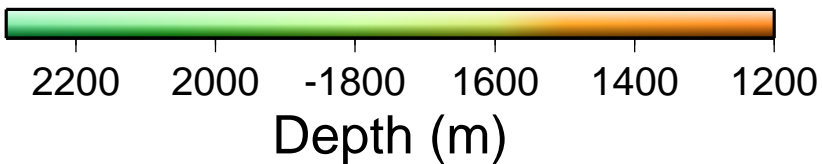
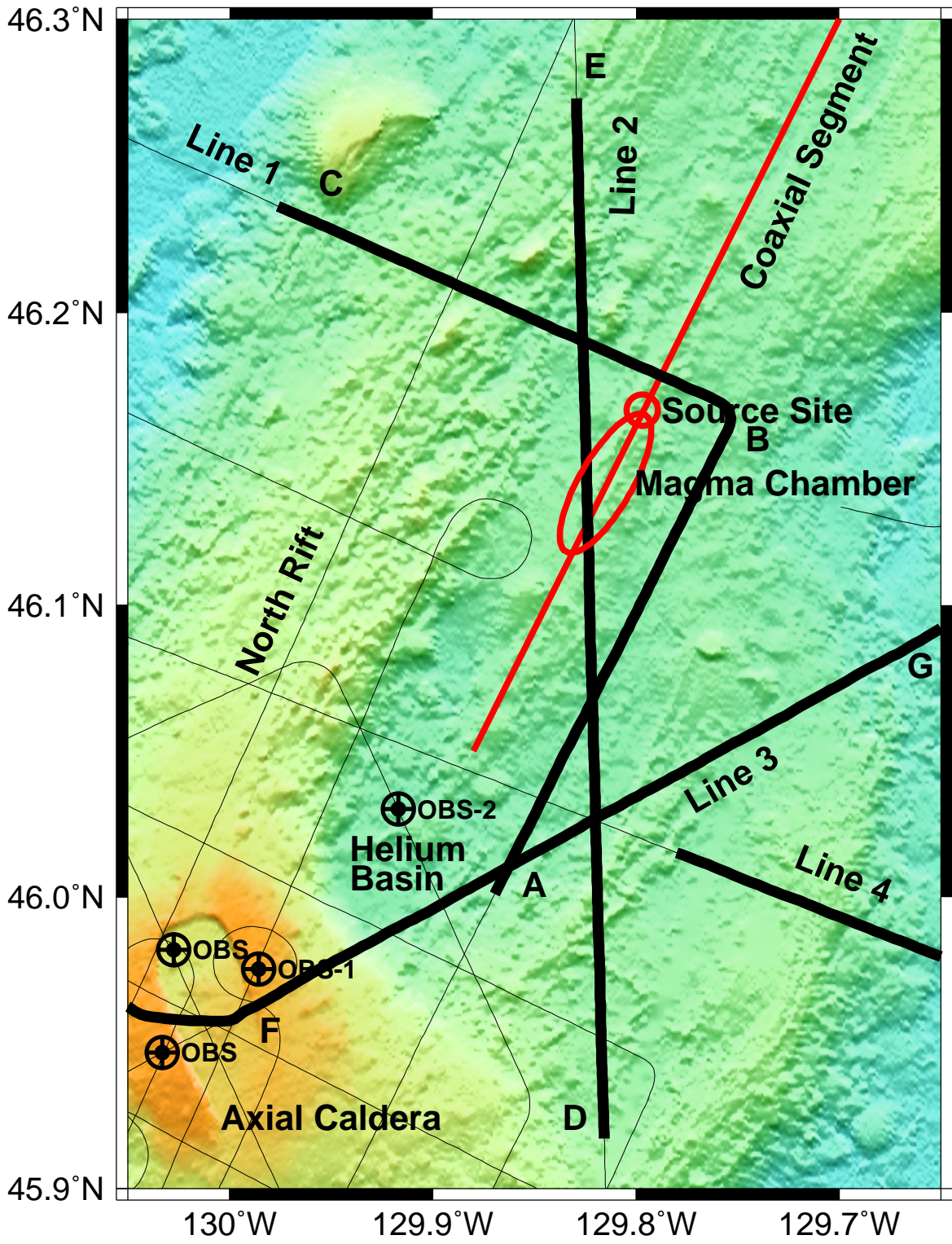
Figure 1. Bathymetric map of Coaxial segment (red line) and Axial volcano (lower left), showing ocean bottom seismometers (OBSs) and lines of airgun shots (light and bold lines). Four lines discussed in text are highlighted in bold. Source site of 1993 eruption and the Coaxial magma chamber are shown in red. Bathymetric data courtesy of National Oceanic and Atmospheric Administration.

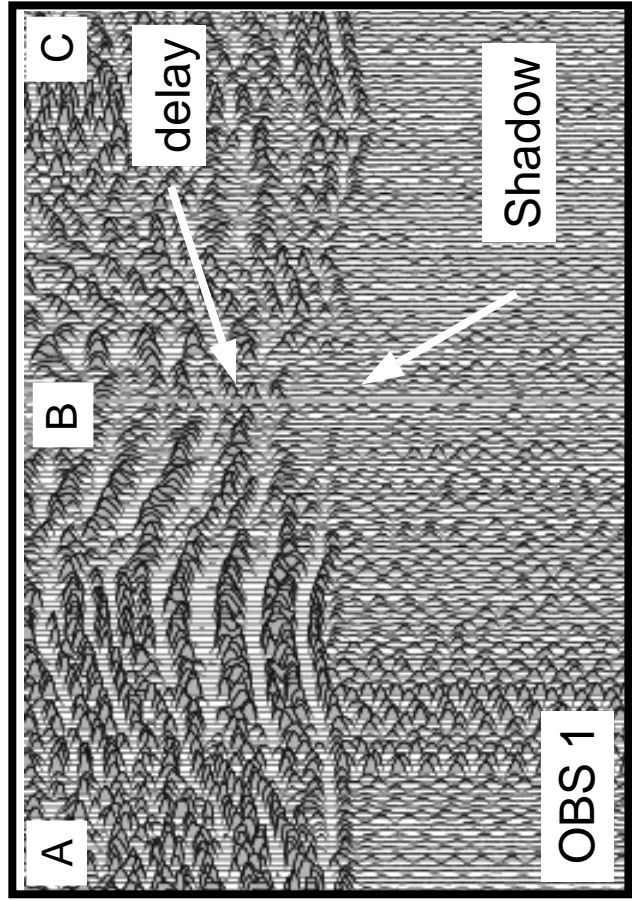
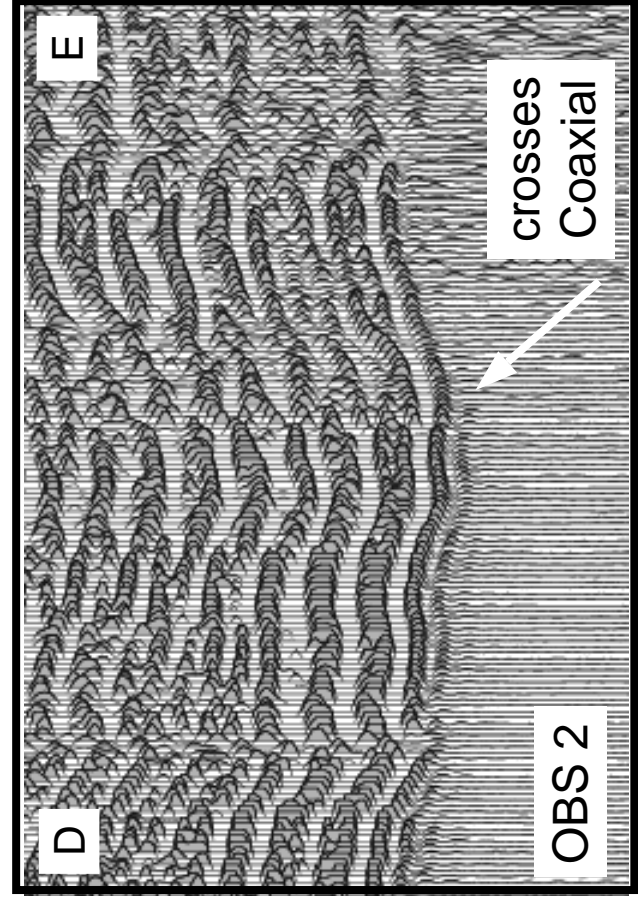
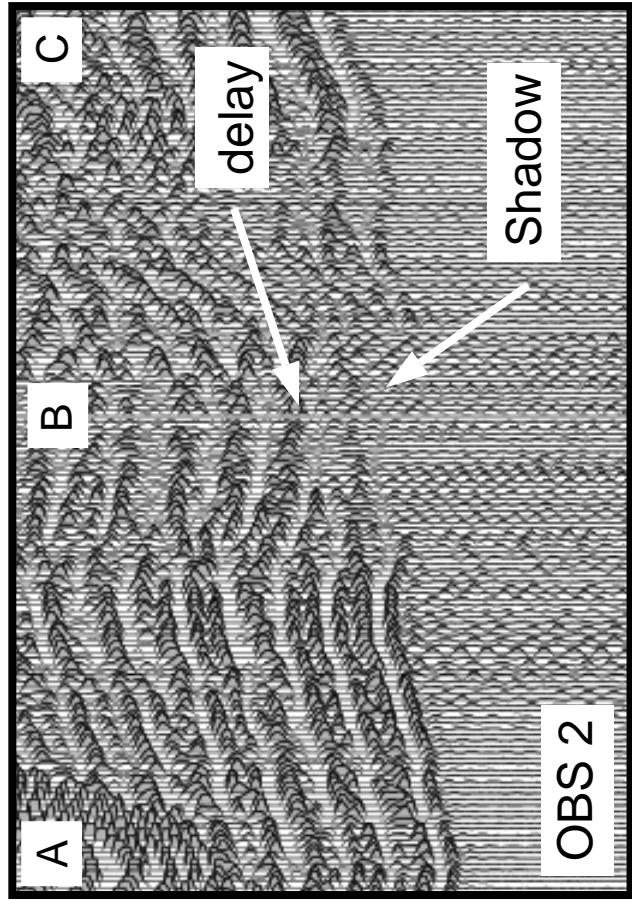
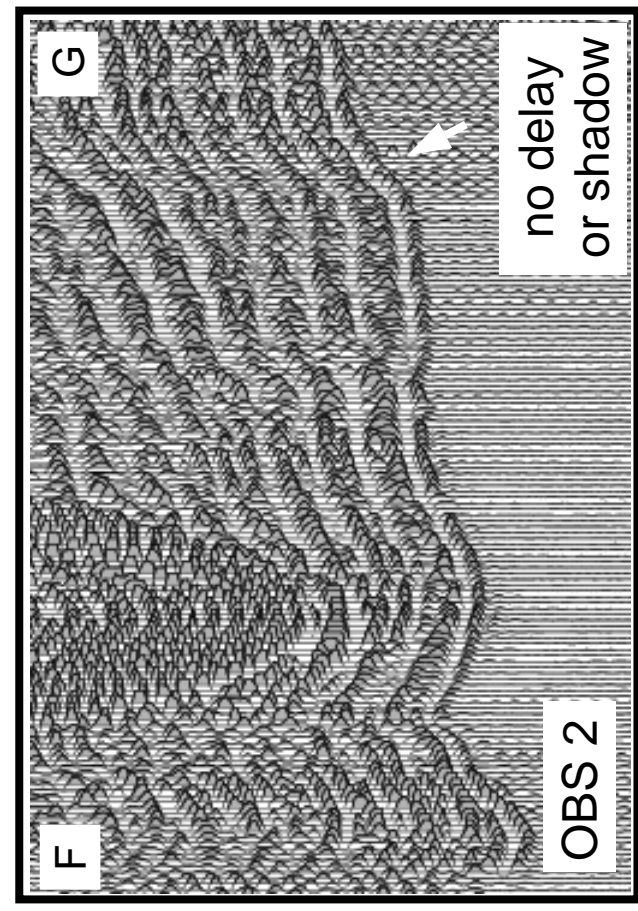
Figure 2. Vertical–component seismic record sections, plotted as a function of distance along the

ship track. Along-track positions marked A through G correspond with those of Fig. 1. The vertical time axis has been reduced by 7 km/s, so that waves with a horizontal phase velocity of 7 km/s plot horizontally. (Bottom left) Line 1 to OBS 1. (Bottom right) Line 1 to OBS 2. Line 1 crosses source site of 1993 Coaxial Eruption. Both OBSs record a prominent delayed arrival associated with a magma chamber beneath source site. (Top left) Line 3 to OBS 2. Line 3 crosses Coaxial segment well south of source site. No delayed arrival is observed. (Top right) Line 2 to OBS 2. Line 2 has about the same source–receiver ranges as does line 1, but does not cross Coaxial segment. No shadowed or delayed arrivals are evident.

Figure 3. Traveltime curves of line 2 to OBS 2 data (solid circles), plotted as a function of distance along the ship track. The vertical time axis has been reduced to 7 km/s, so that waves with a horizontal phase velocity of 7 km/s plot horizontally. Predicted traveltimes (crosses) are for a model with a one-dimensional bathymetrically draped background compressional velocity structure perturbed by a small magma chamber located beneath the source site. A: No magma chamber. B: Magma velocity of 5 km/s. C: Magma velocity of 4 km/s. D: Magma velocity of 3 km/s. A magma velocity of 3 km/s is needed to fit the prominent delayed arrival in the 27–38 km distance range.

Figure 4. Vertical cross sections through three-dimensional compressional velocity model produced by traveltime tomography. A: Cross section along the axis of Coaxial segment. This cross section intersects both Axial volcano and Coaxial segment magma chambers. B: segment–perpendicular cross section. This cross section intersects only the Coaxial magma chamber (MC).





0 36 0 36  
 Distance along track (km) Distance along track (km)

3.5

time-range/7 (s)

1.5

3.5

time-range/7 (s)

1.5

